IAI Journals.ASM.org

The Formins FMNL1 and mDia1 Regulate Coiling Phagocytosis of *Borrelia burgdorferi* by Primary Human Macrophages

Xenia Naj, Ann-Kathrin Hoffmann, Mirko Himmel, Stefan Linder

Institute for Medical Microbiology, Virology and Hygiene, University Medical Center Eppendorf, Hamburg, Germany

Spirochetes of the *Borrelia burgdorferi sensu lato* complex are the causative agent of Lyme borreliosis, a tick-borne infectious disease primarily affecting the skin, nervous system, and joints. During infection, macrophages and dendritic cells are the first immune cells to encounter invading borreliae. Phagocytosis and intracellular processing of *Borrelia* by these cells is thus decisive for the eventual outcome of infection. Phagocytic uptake of *Borrelia* by macrophages proceeds preferentially through coiling phagocytosis, which is characterized by actin-rich unilateral pseudopods that capture and enwrap spirochetes. Actin-dependent growth of these pseudopods necessitates *de novo* nucleation of actin filaments, which is regulated by actin-nucleating factors such as Arp2/3 complex. Here, we demonstrate that, in addition, also actin-regulatory proteins of the formin family are important for uptake of borreliae by primary human macrophages. Using immunofluorescence, live-cell imaging, and ratiometric analysis, we find specific enrichment of the formins FMNL1 and mDia1 at macrophage pseudopods that are in contact with borreliae. Consistently, small interfering RNA (siRNA)-mediated knockdown of FMNL1 or mDia1 leads to decreased formation of *Borrelia*-induced pseudopods and to decreased internalization of borreliae by macrophages. Our results suggest that macrophage coiling phagocytosis is a complex process involving several actin nucleation/regulatory factors. They also point specifically to the formins mDia1 and FMNL1 as novel regulators of spirochete uptake by human immune cells.

Lyme disease, caused by the spirochete *Borrelia burgdorferi*, is the most common tick-borne disease in North America, Europe, and Asia. Infection with borreliae and subsequent spreading of spirochetes to various tissues can result in arthritis or skin disorders and also in Lyme carditis or neuroborreliosis (1–3). At present, 18 *B. burgdorferi sensu lato* genospecies have been identified, five of which are known to cause Lyme disease (*B. burgdorferi sensu stricto*, *B. afzelii*, *B. garinii*, *B. spielmanii*, and *B. bavariensis*) (4).

In the course of the innate immune response to a *Borrelia* infection, professional phagocytes, such as macrophages and dendritic cells, are recruited to sites of infection. Phagocyte uptake of borreliae, as well as their intracellular processing and elimination by professional phagocytes, is thus of critical importance to prevent the dissemination of spirochetes and the development of Lyme disease. Phagocytosis of *B. burgdorferi* has been proposed to proceed through several mechanisms, including CR3-mediated (5–7) and FcγR-mediated phagocytosis (8, 9) (for an overview, see reference 10). Importantly, both Toll-like receptor 2 (TLR2)-dependent and -independent mechanisms have been shown to be essential for phagocytosis of borreliae by peripheral blood mononuclear cells as well as for subsequent cytokine production by these cells (11). The central role of TLR2 has also become evident by use of TLR2 knockout mice, which, compared to wild-type (wt) controls, show increased loads of spirochetes within tissues during the early stages of *Borrelia* infection (12). Signaling events downstream of TLR that are necessary for efficient clearance of spirochetes involve both MyD88 (myeloid differentiation factor 88)-dependent and -independent pathways (6, 10, 13). Moreover, also urokinase receptor has been shown to be involved in phagocytosis and subsequent eradication of borreliae by murine and human leukocytes (14).

Interestingly, the majority of uptake events for *Borrelia* (60% to 70% of all cases [15]) have been described to proceed via coiling phagocytosis. Coiling phagocytosis, initially described for the phagocytic uptake of *Legionella pneumophila* (16), is a unique mechanism, with unilateral pseudopodia enwrapping the bacterial cell. It is an active and selective mechanism, and both living and killed borreliae can be phagocytosed in this manner (15, 17).

Phagocytic uptake of *B. burgdorferi* depends on F-actin polymerization, as shown by blocking experiments with cytochalasin B using neutrophils (18) or cytochalasin D using monocytes (19) or fibroblasts and endothelial cells (20). Furthermore, internalization of *Borrelia* was found to depend on Cdc42 and Rac1 (21), Rho GTPases with major roles in the regulation of actin dynamics during phagocytosis (22, 23). Consistently, downstream effectors of these GTPases, including WASP (*W*iskott-*A*ldrich *s*yndrome *p*rotein) and Arp2/3 complex (24), were shown to localize to pseudopods enwrapping borreliae (21). WASP is an actin nucleation-promoting factor, which activates the Arp2/3 complex (25). Arp2/3 complex is able to induce actin polymerization upon binding to actin filaments, leading to the formation of branched actin networks (26). The essential role of WASP- and Arp2/3 complex-dependent actin polymerization during phagocytosis has been described for a variety of phagocytic processes, including uptake of IgG-coated erythrocytes by murine RAW/LR5 macrophages (27) or both IgG- and C3ib-opsonized beads by J774.A1 mouse macrophages (28). However, this does not exclude the possibility that

Received 12 December 2012 **Returned for modification** 28 December 2012
Accepted 22 February 2013

Published ahead of print 4 March 2013

Editor: R. P. Morrison

Address correspondence to Mirko Himmel, m.himmel@uke.de, or Stefan Linder, s.linder@uke.de.

Supplemental material for this article may be found at http://dx.doi.org/10.1128/IAI.01411-12.

doi:10.1128/IAI.01411-12

other GTPase downstream effectors, and especially those regulating actin filament dynamics, may also play roles during uptake processes in general and specifically in *Borrelia*-induced coiling phagocytosis.

In recent years, proteins of the formin family have emerged as novel regulators of actin filament dynamics (29–32). Like WASP and Arp2/3 complex, formins are effectors of Rho GTPases and were initially described as actin-nucleating proteins (29, 33). It is now recognized that the numerous formin isoforms show great variety in their biochemical properties, which includes actin nucleation, actin filament elongation, filament capping, and severing activity. Formins are multidomain proteins that can be autoinhibited by an intramolecular interaction between their DID and C-terminal DAD domains (34), with the latter also playing a role in actin nucleation (35). From 15 formins expressed in mammalian cells, 3 have so far been implicated in phagocytic processes: mDia1, mDia2 (36), and FMNL1 (37).

FMNL1 is an effector of Cdc42 and Rac1 (37–39). It is expressed in hematopoietic cells and is upregulated in the course of monocyte differentiation to macrophages (40). Alternative splicing of the *FMNL1* gene leads to expression of three isoforms, α, β, and γ, which differ in their C termini (38, 41). Although the exact mechanism of FMNL1 activation is not yet fully understood, several studies demonstrate the involvement of FMNL1 in FcγR-mediated phagocytosis. Accordingly, knockdown experiments in mouse macrophages revealed that the murine FMNL1β homolog (FRLα) is required for phagocytosis of opsonized sheep red blood cells and is recruited to phagocytic cups in a Cdc42-dependent manner (37). In contrast to FMNL1, mDia1 has been linked to CR3-mediated phagocytosis: in RAW 264.7 macrophages, mDia1 is recruited to phagocytic cups that engulf C3ib-opsonized sheep red blood cells (36), and knockdown of mDia1 led to decreased internalization of C3ib- but not IgG-opsonized erythrocytes (36). However, in neutrophils, mDia1 seems to be required for both CR3- and FcγR-mediated phagocytosis (42). Interestingly, mDia formins have also been identified as regulators of filopodium formation in mammalian cells (43).

In the present study, we show that FMNL1 and mDia1 are enriched at macrophage pseudopodia that are induced by and in contact with *Borrelia* spirochetes. This is of crucial functional importance as small interfering RNA (siRNA)-mediated knockdown of either FMNL1 or mDia1 resulted in impaired pseudopod formation and severely reduced phagocytic uptake of *B. burgdorferi* by primary human macrophages.

MATERIALS AND METHODS

Bacterial strains and growth conditions. Wild-type *B. burgdorferi* B31 ATCC 35210 strain (kindly provided by P. Kraiczy) and the previously described green fluorescent protein (GFP)-expressing *B. burgdorferi* B31 5A4 NP1 strain (44) (kindly provided by G. Chaconas) were cultivated in complete Barbour-Stoenner-Kelly H (BSK-H; Sigma-Aldrich, Taufkirchen, Germany) or BSK-II medium prepared in-house (45) containing 6% normal rabbit serum. Genetically modified borreliae were kept under antibiotic selection pressure using 100 μg/ml gentamicin and 200 μg/ml kanamycin. Liquid bacterial cultures were cultivated under microaerophilic conditions at 33°C and ~1% CO_2. For the determination of cell number, morphology, and motility, 10 μl of (diluted) *Borrelia* cultures was filled in a C-Chip Neubauer improved hemocytometer (Digital Bio, Seoul, South Korea) and analyzed by dark-field microscopy using a Zeiss Standard WL upright microscope equipped with a central field stop, a Neofluar 16×/numerical aperture (NA) 0.40/Ph2 objective lens, and two KF 10×/18-mm oculars (Carl Zeiss, Oberkochen, Germany). *Escherichia coli* strain DH5α was used for standard cloning and DNA plasmid amplification procedures. Bacterial cells were grown in LB medium supplemented with 50 μg/ml kanamycin at 37°C and 200 rpm in a shaking incubator.

Plasmid constructs and siRNA. A plasmid encoding enhanced GFP (EGFP)-FMNL1 described by Mersich et al. (40) was kindly provided by S. Blystone (SUNY Upstate Medical University, Syracuse, NY), a yellow fluorescent protein (YFP)-FMNL1 cDNA construct described by Colon-Franco et al. (46) was kindly provided by D. Billadeau (Mayo Clinic, Rochester, MN), pTagRFP (where RFP is red fluorescent protein) (Evrogen, Moscow, Russia), a plasmid encoding Lifeact-mRFP (where mRFP is monomeric RFP) (47), was a kind gift from M. Sixt and R. Wedlich-Söldner (Max Planck Institute for Biochemistry, Munich, Germany), pEGFP-mDia1 and pEGFP-mDia1deltaDAD were obtained from J. Faix (Hannover Medical School, Hannover, Germany), and mCherry-fascin was a kind gift from D. Vignjevic (Institut Curie, Paris, France). The following nucleotide sequence targeting firefly luciferase was used as a negative-control siRNA: 5′-AGGTAGTGTAACCGCCTTGTT-3′ (48). The siRNA against human FMNL1 was On-TargetplusSMARTpool (L-019176; DharmaconRNAi Technologies/Thermo Fisher Scientific, Lafayette, CO); the siRNA sequence against mDia1 was adapted from Goh et al. (49) and humanized [GCUGGUCAGAGCCAUGGAU(dTdT)] (synthesized by Eurofins MWG Operon, Ebersberg, Germany).

Eukaryotic cell culture. Primary human monocytes were isolated from buffy coats (kindly provided by Frank Bentzien, Transfusion Medicine, Universitätsklinikum Hamburg-Eppendorf [UKE], Hamburg, Germany) by centrifugation in Ficoll; 12.5 ml of blood was coated on 15 ml of Ficoll (PromoCell, Heidelberg, Germany) and centrifuged for 30 min at 4°C and 460 × *g*. Leukocyte fractions were transferred in a new 50-ml Falcon tube and filled up to 50 ml with cold RPMI 1640 medium (Invitrogen, Darmstadt, Germany). Cells were washed twice in RPMI 1640 medium and centrifuged for 10 min as described above. Enriched leukocytes were resuspended in 400 μl of monocyte buffer (5 mM EDTA and 0.5% human serum albumin in Dulbecco's phosphate-buffered saline [DPBS], pH 7.4), mixed with 100 μl of a suspension of magnetic beads coupled to CD14 antibodies (Miltenyi, Bergisch Gladbach, Germany), and incubated for 15 min on ice. The mixture was then loaded on an MS+ separation column (Miltenyi, Bergisch Gladbach, Germany) previously placed in a magnetic holder and equilibrated with 500 μl of cold monocyte buffer. Trapped $CD14^+$ monocytes were washed on a column with 500 μl of monocyte buffer and, after the removal of the magnet, eluted with 1 ml of monocyte buffer into 15 ml of cold RPMI 1640 medium. After centrifugation for 10 min at 4°C and 460 × *g*, the supernatant was removed, and cells were resuspended in 40 ml of RPMI 1640 medium and seeded on a six-well plate (Sarstedt, Nümbrecht, Germany) at a density of 1×10^6 cells per well. After adhesion of monocytes, RPMI medium was replaced by 2 ml of monocyte culture medium (RPMI 1640 medium replaced with 15% human serum [prepared in-house] and 100 μg/μl penicillin-streptavidin). Monocytes were cultivated in an incubator at 37°C in 5% CO_2 and 90% humidity; every 3 to 4 days the culture medium was replaced by fresh medium. Monocytes differentiated in 5 to 7 days to macrophages. Subsequent experiments were performed with inactivated and also noninactivated human serum. The two approaches yielded comparable results in regard to filopodium formation and internalization of borreliae.

Transient transfection of primary human macrophages. Primary human macrophages were transiently transfected using a MicroPorator MP-100 device (PeqLab, Erlangen, Germany) and a Neon Transfection System (Invitrogen, Darmstadt, Germany). Prior to transfection, macrophages were detached with Alfazyme (PAA, Pasching, Austria), washed with warm DPBS (Invitrogen, Darmstadt, Germany), and resuspended in buffer R (provided with the Neon Transfection kit). The cell suspension was added to 5 μg of DNA plasmid or 20 μM siRNA. The MicroPorator settings for the transfection were a 1,000-V pulse voltage, 40-ms pulse width, and a pulse number of 2. Immediately after electroporation, mac-

rophages were transferred into prewarmed monocyte buffer and seeded on glass coverslips (Karl Hecht, Sondheim, Germany) or on a glass-bottom dish (Willco Wells, Amsterdam, Netherlands).

Phagocytosis assay. *B. burgdorferi* spirochetes were counted, and 1×10^7 bacterial cells were collected by centrifugation (10 min at 14,000 rpm and 4°C). The supernatant was removed, and the bacteria were resuspended in 500 μl of monocyte cultivation medium. Subsequently, the bacteria suspension was applied on 1×10^5 macrophages and seeded on a coverslip, giving a multiplicity of infection (MOI) of 100. After a given incubation time (as indicated in the figure legends) the bacterial suspension was removed, and macrophages were washed with 1 ml of prewarmed PBS and fixed as described below. For live-cell imaging of phagocytic uptake processes, 1×10^5 macrophages were seeded in a 35-mm dish with a 12-mm glass coverslip in the center (GWSt-3512; Willco Wells, Amsterdam, Netherlands) and incubated with *B. burgdorferi* at an MOI of 100.

A double-fluorescence staining method was applied to distinguish between extracellular (adherent) and intracellular (internalized) *Borrelia burgdorferi*. Extracellular bacteria were stained after fixation of specimens (4% paraformaldehyde and blocking for 30 min with 10% normal goat serum/normal human serum [NGS/NHS] in PBS) with primary antibody Bss42 (dilution of 1:1,000) and secondary anti-mouse antibody coupled to Alexa Fluor-568 (dilution of 1:200). Internalized borreliae were stained after subsequent permeabilization (0.5% Triton X-100 in PBS) and a second treatment with primary and secondary antibodies, the latter labeled with Alexa Fluor-488. Extracellular borreliae thus appear yellow (merge of red and green), while intracellular borreliae are stained only in green. For each condition, 30 cells associated with borreliae were analyzed, with experiments performed in triplicate using macrophages from three different donors.

Immunoblotting. Proteins were separated by SDS-polyacrylamide gel electrophoresis and blotted onto nitrocellulose membrane using an iBlot dry blotting system (Invitrogen, Darmstadt, Germany) with blotting program P2. After transfer, the membrane was rinsed in PBS and incubated for 30 min in blocking solution (5% milk powder in PBS–0.05% Tween 20 [PBST] or in Tris-buffered saline [TBS]–0.01% Tween 20 [TBST]). Dilutions of primary antibodies were prepared in 5% milk powder (wt/vol) in PBST (anti-FRL1 and anti-fascin) or in 3% bovine serum albumin (BSA; wt/vol) in TBST (anti-mDia1), and the membrane was incubated overnight at 4°C. After three washing steps in PBST or TBST, the membrane was incubated at room temperature for 1 h in dilutions of goat anti-mouse or anti-rabbit IgG secondary antibodies conjugated to horseradish peroxidase (Dianova, Hamburg, Germany). Enhanced chemiluminescence was used for the detection of bound antibodies: after three washing steps in PBST or TBST, the membrane was immersed in freshly prepared detection solution (SuperSignal West Femto; Pierce/Thermo Fisher Scientific, Rockford, IL), and chemiluminescence signals were collected on an X-ray film (Fujifilm, Düsseldorf, Germany), which was developed and fixed in an automatic processing machine (Agfa Curix 60; Agfa HealthCare, Bonn, Germany).

Immunostaining and fluorescence microscopy. Antibodies and staining reagents used in this study were Arp2 (IgG1 mouse monoclonal antibody) (ab49674; Abcam, Cambridge, United Kingdom), Bss42 (IgG2a mouse monoclonal antibody) (NB110-8005; Novus Biologicals, Cambridge, United Kingdom), anti-fascin (mouse monoclonal antibody) (ab78487; Abcam, Cambridge, United Kingdom), anti-FRL1 (rabbit polyclonal antibody to FMNL1, kindly provided by H. Higgs, Dartmouth College, NH), mDia1 (IgG1 mouse monoclonal antibody) (610848; BD Biosciences, Heidelberg, Germany), phalloidin conjugated to Alexa Fluor-488, -568, or -647 (Invitrogen, Darmstadt, Germany), and goat anti-mouse or goat anti-rabbit IgG secondary antibodies conjugated to Alexa Fluor-488 or -568 (Invitrogen, Darmstadt, Germany). Wild-type borreliae were visualized by staining DNA with Hoechst 33342 fluorescent dye (A0741; AppliChem, Darmstadt, Germany).

Macrophages seeded at a density of 10^5 cells per glass coverslip were fixed for 10 min in prewarmed 3.7% formaldehyde-PBS, washed three times in PBS, and permeabilized for 10 min in 0.5% Triton X-100–PBS. After being washed with PBS, cells were incubated for 30 min in blocking solution (10% normal goat serum and normal human serum in PBS), briefly washed in PBS, and incubated for 30 to 60 min in a primary antibody solution. Cells were washed three times in PBS and then incubated for 30 min in secondary antibody solution supplemented with fluorescently labeled phalloidin, as indicated in the figure legends. After three washing steps in PBS, coverslips were finally dipped twice in distilled water, excessive liquid was carefully removed with tissue paper, and the coverslip was mounted in a small volume of Mowiol 4-88 supplemented with diazabicyclooctane (DABCO) antibleaching reagent (Carl Roth, Karlsruhe, Germany) on a microscope slide. The mounting medium hardened overnight, and stained samples were stored at +4°C protected from light. For image acquisition, confocal laser scanning microscopy was performed using a Leica TCS SP2 AOBS microscope equipped with an HCX PL APO 63× (NA 1.4 to 0.60) lambda blue oil immersion objective lens (Leica, Mannheim, Germany) and one multi-Ar laser (488-nm line) as well as two HeNe lasers (543-nm and 633-nm lines). Confocal *Z*-stacks were acquired using a motorized piezoelectric *Z*-drive and a step size of 0.123 μm.

Live-cell imaging. High-speed live-cell imaging was performed using two different spinning-disk microscopes: an Improvision spinning-disk microscope system controlled by Volocity, version 4.3.1, software and based on an Axiovert 200 M stand equipped with a Plan-Apochromat 63×/NA 1.4 oil immersion objective lens (Carl Zeiss, Jena, Germany) and a CSU-22 spinning-disk unit (Yokogawa, Tokyo, Japan) with an electron-multiplying charge-coupled-device (EM-CCD) camera (C9200-50; Hamamatsu Photonics, Hamamatsu City, Japan) and an environmental chamber for controlling temperature, humidity, and CO_2 levels (Solent Scientific, Segensworth, United Kingdom). Movies were corrected for acquisition photobleaching and further processed using Volocity software (PerkinElmer, Waltham, MA).

For live-cell imaging of Lifeact-mRFP-expressing cells, primary human macrophages were transiently transfected using a MicroPorator MP-100 device (PeqLab, Erlangen, Germany). A total of 1×10^6 cells were transfected with 5 μg of Lifeact-mRFP plasmid DNA using the following parameters: 1,000-V pulse voltage, 40-ms pulse width, and a pulse number of 2.

Ratiometric fluorescence microscopy. For ratiometric live-cell imaging, an UltraViewVoX spinning-disk microscope system (PerkinElmer, Waltham, MA) was used. The system was based on a Axio Observer Z.1 stand equipped with a Plan-Apochromat 63×/NA 1.4 differential interference contrast (DIC) oil immersion objective lens (Carl Zeiss, Jena, Germany), a CSU X-1 spinning-disk unit (Yokogawa, Tokyo, Japan), an EM-CCD camera (C9200-50; Hamamatsu Photonics, Hamamatsu City, Japan), and a small environmental chamber for controlling temperature, humidity, and CO_2 levels, combined with an objective lens heater (Tokai Hit, Japan). Using Volocity, version 6.1, software (PerkinElmer), ratiometric images were created by dividing background-corrected signal intensities from EGFP fluorescence by signal intensities from TagRFP fluorescence for each pixel. Resulting ratios were represented by a rainbow colors ranging from blue (ratio equals 1.0) to red (ratio values as indicated in Fig. S1 in the supplemental material).

Ratiometric calculation. Fluorescence signal intensities at phagocytic uptake structures or in control regions in the cytoplasm were determined using Volocity software (PerkinElmer). Several regions of interest were selected, and mean gray values were used for further calculations. In order to compare fluorescence signal intensities obtained from different cells and expression constructs, signal intensity ratios were normalized to overall fluorescence intensities for the two fluorophores (EGFP and TagRFP) as follows. The ratio of fluorescence intensities at phagocytic uptake structures, calculated as Rp = EGFP/TagRFP, was divided by the ratio of fluorescence intensities in the cytoplasm, calculated as Rc = EGFP/TagRFP (averaged for three different cytoplasmic locations with no apparent en-

richment of EGFP-tagged formin constructs). For the analysis of specific protein enrichments at phagocytic uptake structures, a recruitment index, Ri, was calculated as Rp/Rc (37).

Statistical analysis. Statistical evaluation of the obtained data sets was performed in Prism, version 5.0d, for Mac (GraphPad Software, La Jolla, CA) using a two-tailed Student's *t* test. Results are presented as means ± standard errors means (SEM).

RESULTS

Dynamic F-actin-rich pseudopodia are involved in the phagocytic uptake of *B. burgdorferi* by primary human macrophages. Coiling phagocytosis has been described as the predominant uptake mechanism for *B. burgdorferi* spirochetes by immune cells (15, 50). Detailed analysis of this phenomenon, however, has so far been limited to fixed specimens (15, 17, 50, 51). To clarify the dynamics of coiling phagocytosis, we used confocal laser scanning microscopy and imaged the phagocytic uptake of *B. burgdorferi* spirochetes expressing GFP by primary human macrophages that express the F-actin probe Lifeact-mRFP (47). Proof-of-principle experiments using high-resolution confocal microscopy of fixed samples show that primary macrophages coincubated with GFP-expressing *B. burgdorferi* extend elongated pseudopodia that repeatedly wrap around spirochetes, which is a hallmark of coiling phagocytosis (Fig. 1A) (15). Expression of Lifeact-mRFP demonstrated that these pseudopodia are enriched in F-actin, which is consistent with previous observations (21).

Next, we performed high-speed spinning-disk microscopy to monitor the dynamics of the *B. burgdorferi* uptake by living human macrophages (Fig. 1B; see also Video S1 in the supplemental material). Similar to the observations with fixed samples (Fig. 1A), macrophages in contact with borreliae formed prominent coiling pseudopodia that were enriched in F-actin (Fig. 1B). Tracking over time revealed that these pseudopodia are highly dynamic and enwrap trapped spirochetes in a growing number of coils (Fig. 1B′). Wrapping by pseudopodia proceeded simultaneously with internalization of spirochetes, with internalized parts of borreliae mostly adopting a circular morphology (Fig. 1B′). These experiments show that coiling phagocytosis of borreliae by primary macrophages is driven by F-actin-rich pseudopodia, which capture spirochetes and progressively enwrap them until internalization is complete.

Arp2/3 complex and the formins FMNL1 and mDia1 localize at *Borrelia*-contacting protrusions. The pronounced accumulation of F-actin at *Borrelia*-enwrapping pseudopodia indicated the necessity for actin nucleation processes within these structures. Indeed, using immunofluorescence, we detected enrichment of Arp2, a subunit of the actin-nucleating Arp2/3 complex, at pseudopodia (Fig. 2A to C). This is consistent with earlier observations of dot-like accumulations of Arp2/3 complex along *Borrelia*-containing coiling structures (21). However, Arp2/3 complex is mostly involved in the generation of branched actin networks, which occur in lamellipodia (52, 53), or at phagocytic cups (28). We therefore asked whether other actin nucleation factors might be involved in the generation of actin filaments within *Borrelia*-contacting pseudopodia. We focused particularly on members of the formin family, which induce formation of unbranched actin filaments (54–56).

Especially two members of the formin family are known to be involved in phagocytic processes: FMNL1, which acts in FcγR-mediated phagocytic cup formation in RAW 264.7 cells (37), and mDia1, which is involved in CR3-mediated phagocytosis uptake of erythrocytes by a macrophage cell line (22). We therefore analyzed the subcellular localization of FMNL1 and mDia1 in primary human macrophages coincubated with *B. burgdorferi*. Immunofluorescence staining revealed that both endogenous FMNL1 and mDia1 are enriched at elongated protrusions of macrophages that are in contact with borreliae (Fig. 2D to F and G to I). Distribution of FMNL1 and mDia1 within these protrusions was not uniform, with FMNL1 being localized at the tips and also along the whole length of the protrusions (Fig. 2D) and mDia1 being mostly localized at the tips of these structures (Fig. 2G). We conclude from these findings that FMNL1 and mDia1 are specifically enriched at elongated pseudopodia of macrophages that contact borreliae.

FMNL1 and mDia1 are enriched at dynamic filopodia of living macrophages. To clarify the nature of the macrophage protrusions contacting borreliae and to analyze their dynamic behavior, we used macrophages expressing the filopodium marker fascin fused to mCherry. Cells also coexpressed either EGFP-fused FMNL1 (isoform β) (Fig. 3A) or mDia1, fused to EGFP (Fig. 3B), to label *Borrelia*-induced protrusions. (Note that in the case of mDia1, we used both a full-length construct and a nonautoinhibited form lacking the C-terminal DAD domain [mDia1ΔDAD]. Observed localizations for both constructs were identical [see Fig. S1 in the supplemental material] although the number of protrusions per cell was sometimes increased in case of the mDia1ΔDAD construct.) Importantly, mCherry-fascin decorated almost the entire length of the *Borrelia*-induced protrusions and was absent only from the tip of the structures (Fig. 3A). EGFP-FMNL1β was present along the entire length of the protrusions, including the fascin-free tip (Fig. 3A), while EGFP-mDia1ΔDAD decorated mostly the tips of the protrusions (Fig. 3B). Moreover, the protrusions positive for mCherry-fascin and mEGFP-FMNL1 or EGFP-mDia1ΔDAD were found to be highly dynamic and to extend by several micrometers within a few minutes (Fig. 3A′). We conclude from these findings that *Borrelia*-induced protrusions contain the filopodium marker protein fascin and show dynamics that are consistent with filopodial growth, as observed earlier for melanoma and neuroblastoma cells (57–59). Collectively, *Borrelia*-induced protrusions of macrophages thus qualify as bona fide filopodia.

Especially in case of EGFP-mDia1 (both the full-length or ΔDAD construct), we noted an apparent enrichment at the tips of *Borrelia*-induced filopodia (Fig. 3B and B′; see also Fig. S1A to E in the supplemental material). To quantify this enrichment, we next performed ratiometric fluorescence microscopy of cells expressing EGFP or EGFP-mDia1, together with TagRFP (see Fig. S1F to I). The isolated fluorescence tags (TagRFP and EGFP) showed a mostly diffuse distribution in the cell upon overexpression, resulting in an intensity ratio (EGFP/TagRFP) of 1.01 ± 0.02 (Fig. 1I). In contrast, the intensity ratio for EGFP-mDia1 at filopodial tips (see Fig. S1F and G) were significantly higher, being 3.72 ± 0.49. We conclude from these measurements that EGFP-mDia1 is specifically enriched at filopodium tips of macrophages that were stimulated by cocultivation with borreliae.

Moreover, cultivation of macrophages (i) under standard cell culture conditions, (ii) with supernatants from *Borrelia* cultures, or (iii) with whole borreliae showed that macrophages form some filopodia per cell under normal culture conditions (1.2 ± 0.2 filopodia) (Fig. 3C) and also upon culturing with *Borrelia* super-

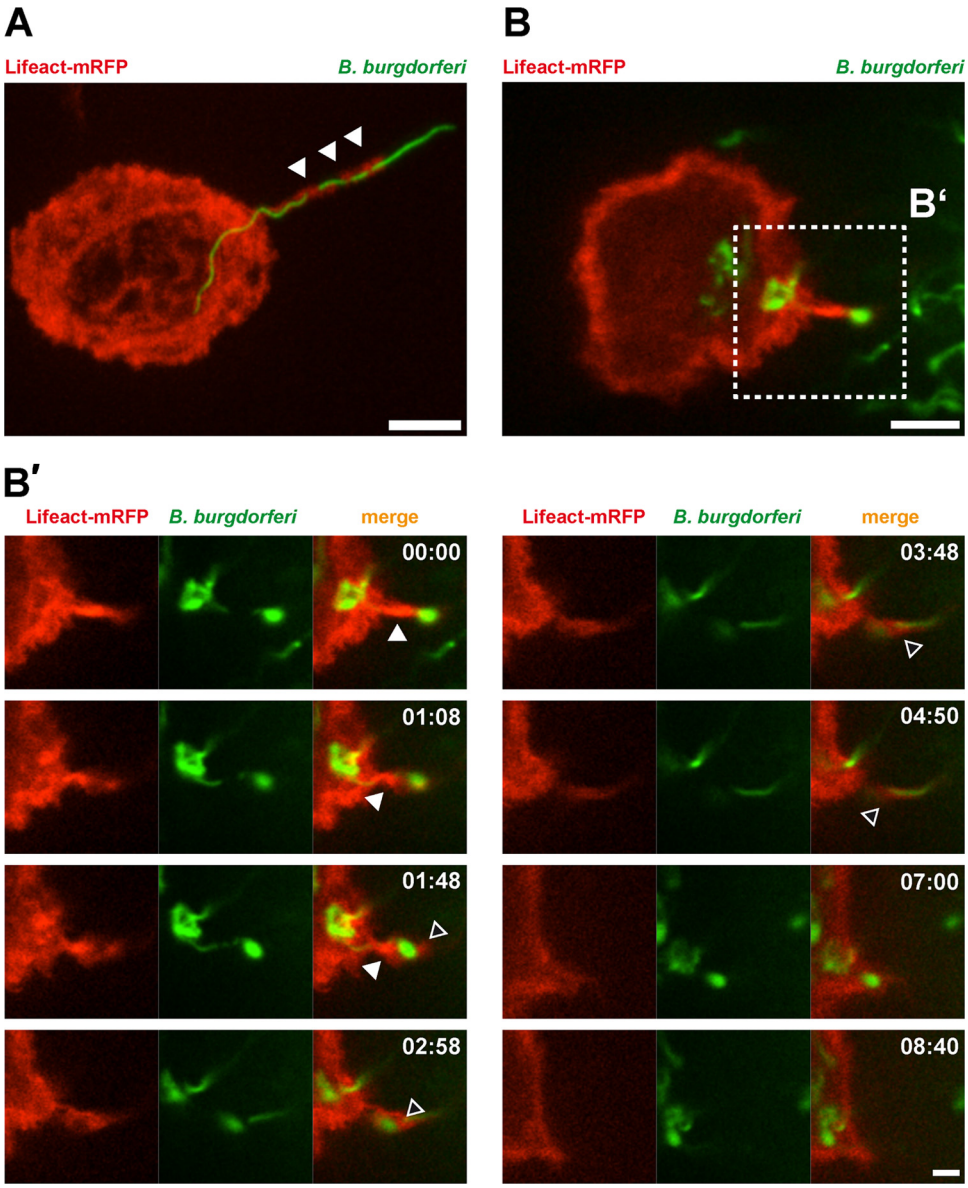

FIG 1 Formation of F-actin-rich uptake structures during coiling phagocytosis of *Borrelia burgdorferi* by primary human macrophages. (A and B) Confocal laser scanning micrographs of primary macrophages expressing Lifeact-mRFP (for labeling F-actin; red), in contact with GFP-expressing *B. burgdorferi* spirochetes (green). (A) Fixed specimen. Note the alteration between F-actin-rich pseudopod coils (arrowheads) and a spirochete enwrapped by a pseudopod. Scale bar, 5 μm. (B) Live-cell microscopy of *Borrelia* uptake. Still frames from Video S1 in the supplemental material are shown. The white box indicates the area enlarged in the images shown in B′. Note the formation of several F-actin-rich coils of the pseudopodium enwrapping the spirochete (individual coils tracked by open and filled arrowheads, respectively) and eventual complete uptake of the spirochete into the macrophage cell. Time from the start of the experiment is indicated as min:sec. Scale bar, 2 μm.

natants (data not shown), but overall formation of filopodia was greatly increased upon coculture with whole borreliae (Fig. 3A and B). To address the question whether borreliae have to be viable in order to induce filopodium formation, we quantified both the number of filopodia per cell and also filopodium length, each time in response to addition of live or heat-killed borreliae to macrophage cultures. Both live and dead borreliae induced comparable numbers of filopodia (3.0 ± 0.2 filopodia for live borreliae, 3.1 ± 0.3 for dead borreliae, and 1.2 ± 0.2 for unstimulated macrophages) (Fig. 3C), which were also of similar lengths (6.2 μm ± 0.4 μm for live borreliae, 6.2 μm ± 0.4 μm for dead borreliae, 3.2 μm ± 0.3 μm for unstimulated macrophages) (Fig. 3D). We conclude that contact of macrophages with whole borreliae, either live or heat-killed, leads to increased filopodium formation.

Knockdown of FMNL1 or mDia1 impairs filopodium formation and *B. burgdorferi* internalization. The prominent localization of both FMNL1 and mDia1 to *Borrelia*-induced filopodia implied that both formins might influence the formation or upkeep of these structures and thus the capturing and eventual internalization of spirochetes. To investigate the possible functional relevance of FMNL1 and mDia1 in filopodium formation, we established siRNA-induced knockdowns of these pro-

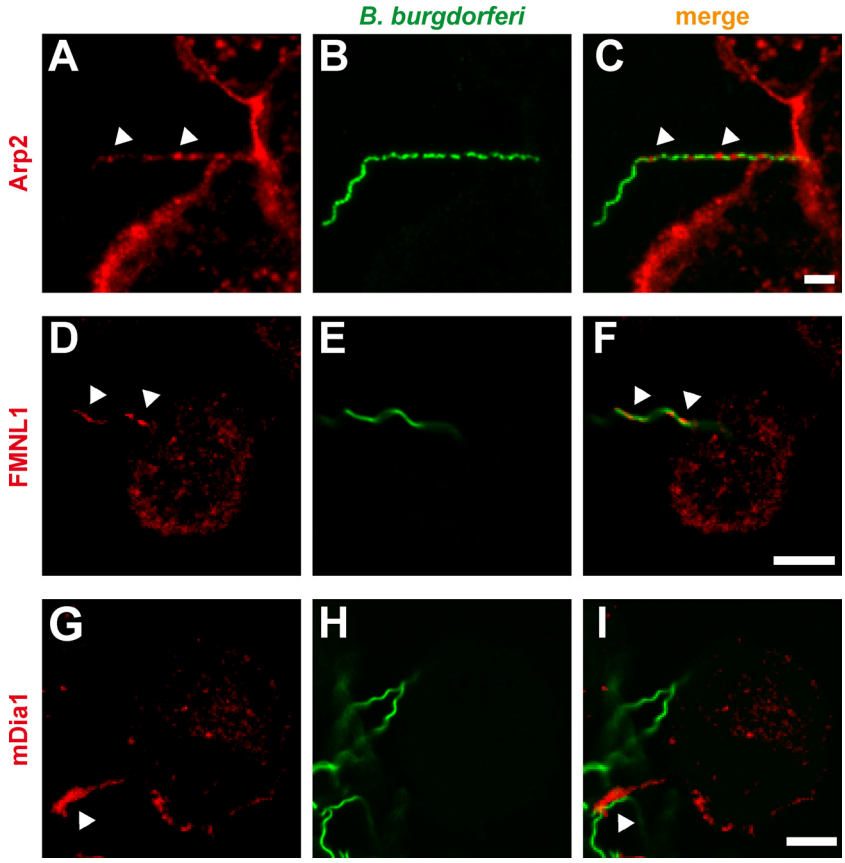

FIG 2 (A to I) Localization of Arp2/3 complex and the formins FMNL1 and mDia1 at *B. burgdorferi*-containing uptake structures of macrophages. Confocal immunofluorescence micrographs of primary human macrophages coincubated with GFP-expressing *B. burgdorferi* spirochetes and stained for endogenous proteins using specific primary antibodies. Note the accumulation of the Arp2/3 complex subunit Arp2, of FMNL1, and of mDia1 in macrophage pseudopodia (arrowheads in first and third columns) which contact borreliae. Scale bar, 5 μm.

teins. Transfection of macrophages with respective siRNAs led to a pronounced decrease of ~80% for FMNL1 after 3 days and of ~73% for mDia1 after 2 days (Fig. 4A). We then performed a coincubation assay with siRNA-treated macrophages and analyzed the formation of *Borrelia*-induced filopodia. The number of macrophages showing filopodia that were in contact with spirochetes was set to 100% (note that at a given time point, mostly only one *Borrelia* cell was found to be in contact with a macrophage cell). Strikingly, knockdown of FMNL1 resulted in a ca. 50% reduction of *Borrelia*-contacting filopodia, while knockdown of mDia1 resulted in a 75% reduction (Fig. 4B). These results indicate that FMNL1 and mDia1 are necessary for the formation of filopodia in macrophages cocultured with borreliae.

As borreliae are to a significant degree internalized by coiling phagocytosis (15) and as filopodium formation appears to be a prerequisite for this process, we next analyzed the potential impact of FMNL1 and mDia1 knockdown on the internalization of borreliae by macrophages. For this, macrophages were transfected with respective siRNAs for FMNL1 and mDia1, incubated for 3 days and 2 days, respectively, and cocultured with borreliae (at an MOI of 100) for 1 h. To distinguish between internalized and noninternalized spirochetes, specimens were processed using an outside/inside staining protocol, resulting in double labeling (red and green) of noninternalized and single labeling (green) of internalized borreliae (Fig. 4C to J). Strikingly, knockdown of either protein resulted in a clear reduction of internalized spirochetes (phagocytic index for FMNL1 siRNA-treated cells, 0.38 ± 0.10; phagocytic index for mDia1 siRNA-treated cells, 0.22 ± 0.02; phagocytic index for luciferase siRNA-treated control cells, 0.94 ± 0.14), corresponding to a decrease in uptake of 60% for FMNL1 siRNA-treated cells and of 77% for mDia1 siRNA-treated cells (Fig. 4K).

In order to quantify the relative proportion of coiling phagocytosis for *Borrelia* uptake by macrophages, we evaluated fixed specimens of borreliae in contact with macrophages. Only borreliae enwrapped in several, clearly recognizable whorls were counted as bona fide coiling phagocytosis events. This evaluation excluded all other uptake events, i.e., (i) borreliae attached to filopodia but not yet enwrapped, (ii) borreliae taken up via coiling phagocytosis but without clearly recognizable whorls, or (iii) borreliae directly taken up at the surface without a coiling intermediate. Approximately 30% of cell-attached borreliae were found to be associated with multiple whorls on the macrophage surface, and this value was reduced to ca. 13% upon knockdown of either FMNL1 or mDia1 (Fig. 4L). These data indicate that (i) both FMNL1 and mDia1 are necessary for efficient phagocytic uptake of *B. burgdorferi* by primary human macrophages and (ii) a significant proportion of FMNL1- and mDia1-mediated uptake events proceeds through coiling phagocytosis.

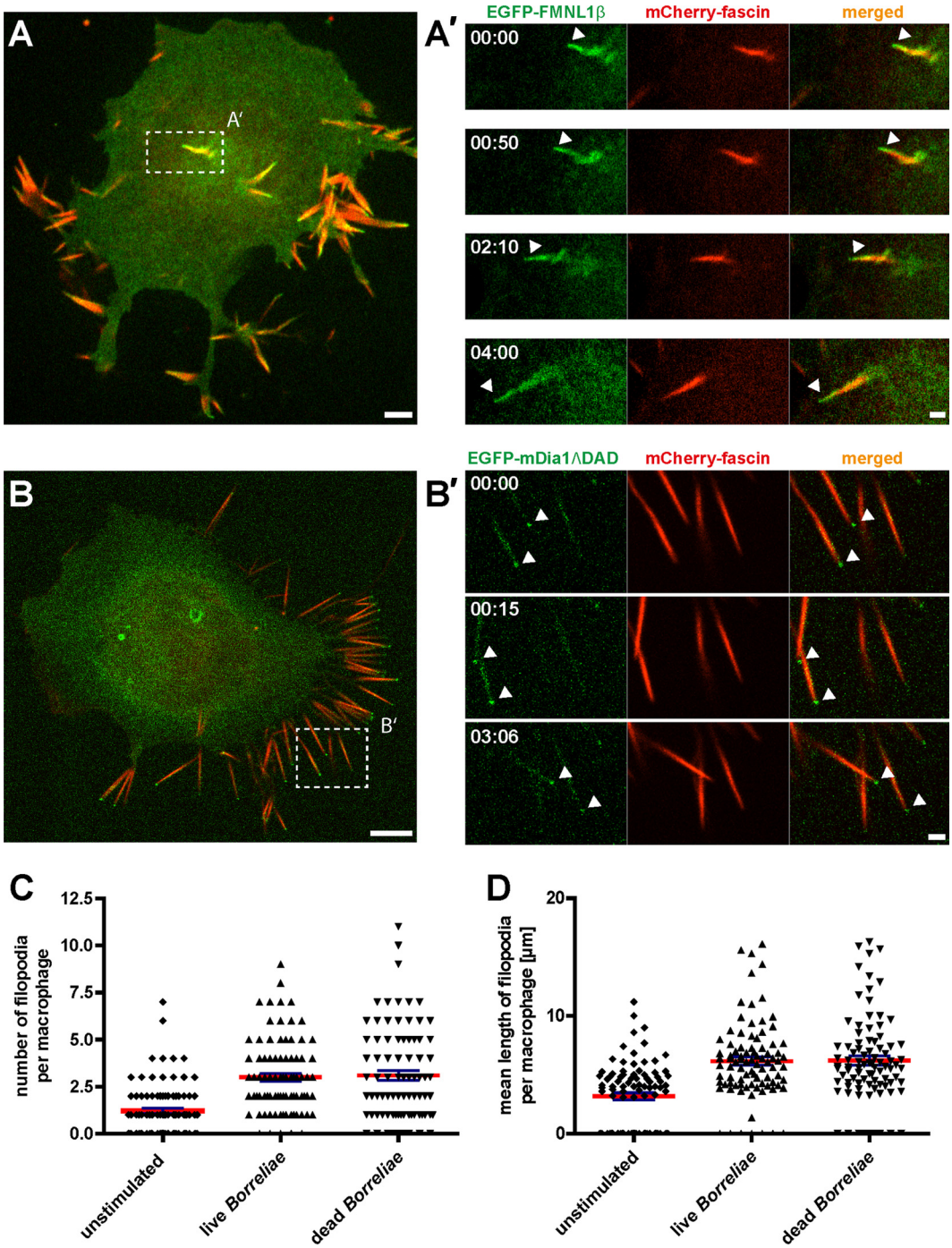

FIG 3 *Borrelia*-stimulated macrophage pseudopodia are enriched in EGFP-FMNL1β or EGFP-mDia1ΔDAD and are positive for the filopodium marker fascin. Confocal micrographs of macrophages expressing mCherry-fascin (red) and EGFP-FMNL1β (green; A) or EGFP-mDia1ΔDAD (green; B). (A and B) Still images from Videos S2 and S3 in the supplemental material. Dashed white boxes indicate the areas enlarged in the images shown in panels A′ and B′. Note localization of EGFP-FMNL1β along the length of filopodia, including the fascin-free tip (arrowhead), and its persistence over time (A′). Note the localization of EGFP-mDia1ΔDAD especially at the tips of filopodia (arrowheads) (B′). Scale bar, 2 μm. Time from the start of the experiments is indicated as min:sec. (C and D) Evaluation of number and length of filopodia in unstimulated macrophages and macrophages stimulated by addition of either live or heat-killed borreliae. To distinguish between microspikes and filopodia, only protrusions with a length of >3 μm were evaluated. Values are given as means ± SEM.

DISCUSSION

In this study, we investigated the mechanisms of coiling phagocytic uptake of borreliae by primary human macrophages. Previous studies indicated the crucial involvement of actin polymerization in this process. First, formation of protrusions from neutrophils and subsequent internalization of borreliae were found to be dependent on actin polymerization, as shown by inhibition experiments using cytochalasin B (18) or cytochalasin D (19, 20). Second, actin-

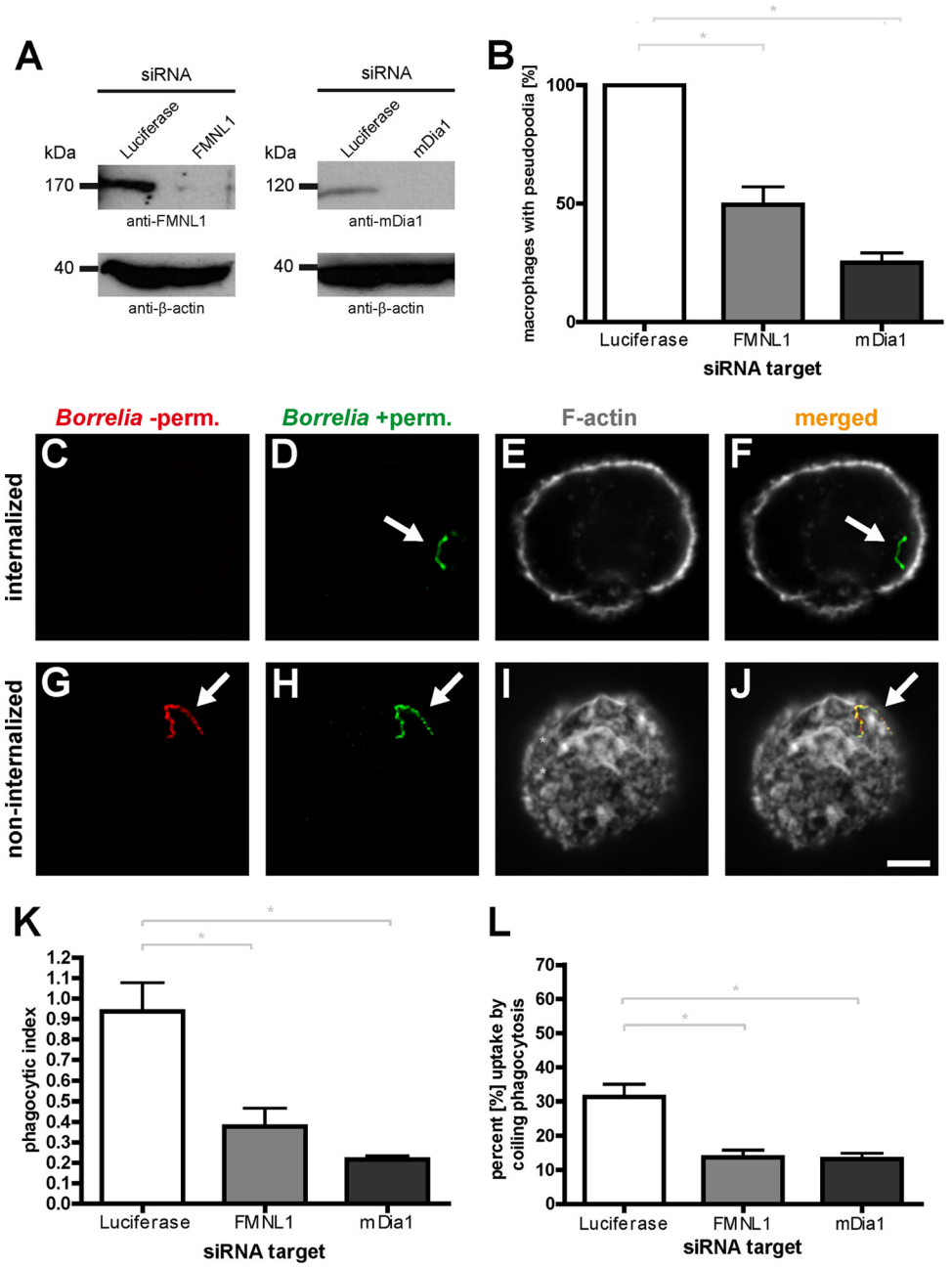

FIG 4 siRNA-induced depletion of FMNL1 or mDia1 impairs the internalization of *B. burgdorferi* by primary human macrophages. (A) Western blots of lysates from macrophages treated with luciferase-specific siRNA (as a control), FMNL1-specific siRNA (left blot) or mDia1-specific siRNA (right blot). Proteins were detected with specific antibodies, with β-actin used as a loading control. Molecular mass in kDa is indicated. (B) Quantification of *Borrelia*-induced pseudopodia. The number of macrophages with pseudopodia in control cells treated with luciferase siRNA was set to 100%. Note the pronounced reduction of pseudopodium formation in cells depleted of FMNL1 or mDia1. Values are shown as means ± SEM (*, $P < 0.05$). The proportions of macrophages with pseudopodia are 49.6% ± 7.6% for FMNL1 siRNA and 25.1% ± 4.2% for mDia1 siRNA. For each value, each time 30 cells from three different donors were evaluated in three independent experiments. (C to J) Principle of outside-inside staining. Confocal laser scanning micrographs of macrophages coincubated with borreliae. To distinguish between internalized and noninternalized spirochetes, specimens were fixed and not permeabilized (−perm), stained with Bss42 *B. burgdorferi* antibody and with Alexa Fluor 568-labeled secondary antibody (red; C and G), and subsequently permeabilized (+perm) and stained with the same primary antibody but with Alexa Fluor 488-labeled secondary antibody (green; D and H). Internalized borreliae are detected only by the second round of staining and appear green; borreliae on the outside of the macrophages are detected by both stainings (red and green) and appear yellow in the merged image (F and J). Macrophages were stained with Alexa Fluor 647-labeled phalloidin to detect F-actin (E and I). Scale bar, 5 μm. (K) Internalization of borreliae by macrophages treated with specific siRNAs, based on evaluation of respective outside-inside staining. The phagocytic index is indicated as the ratio of internalized to noninternalized spirochetes. Values are given as means ± SEM (*, $P < 0.05$). Note the pronounced reduction of the phagocytic index upon depletion of either FMNL1 or mDia1 (phagocytic index of 0.38 ± 0.1 for FMNL1 siRNA and 0.22 ± 0.02 for mDia1 siRNA). For each value, each time 30 cells from three different donors were evaluated in three independent experiments. (L) Coiling phagocytosis of borreliae is reduced upon knockdown of FMNL1 or mDia1. Fixed specimens of borreliae in contact with macrophages were evaluated for the presence of several, clearly recognizable whorls enwrapping spirochetes as an indicator for coiling phagocytosis. Values are given as means ± SEM (*, $P < 0.05$). The percentages of uptake by coiling phagocytosis were 31.2% ± 6.5% for control macrophages transfected with luciferase siRNA, 13.7% ± 3.7% for macrophages transfected with FMNL1-specific siRNA, and 13.3% ± 2.9% for macrophages transfected with mDia1-specific siRNA. For the numbers of attached spirochetes per macrophage cell, see Fig. S3 in the supplemental material.

nucleating Arp2/3 complex has been localized to coiling pseudopods of fixed macrophages that enwrap *B. burgdorferi* (21), indicating a requirement for *de novo* assembly of F-actin during coiling phagocytosis.

Using macrophages that express the F-actin probe Lifeact (47) and GFP-expressing borreliae (44), we demonstrate here for the first time the dynamics of coiling phagocytosis in living cells. F-actin-rich protrusions were found to contact and successively enwrap captured borreliae in a growing number of coils, with continuous internalization of the spirochete until full uptake had been achieved. These observations clearly demonstrate that actin dynamics are involved in the phagocytosis of borreliae, confirming earlier results (18, 21). Coexpression of the filopodium marker fascin (60–62) identified the initial *Borrelia*-capturing protrusions as filopodia. In addition, our finding that filopodium formation by macrophages is increased upon coculture with whole borreliae but not with medium from *Borrelia* cultures is in line with earlier findings showing that protrusion/filopodium induction of human monocytes requires whole bacterial cells and cannot be triggered by soluble factors from *Borrelia* culture supernatants or spirochete fragments obtained by sonication (63). The pseudopods enwrapping spirochetes during coiling phagocytosis are thus mostly not preexisting but are formed by macrophages that encounter intact spirochete cells (15, 17, 50). Moreover, the observation that filopodia are induced by both live and heat-killed borreliae is consistent with previous reports showing coiling phagocytosis of both viable and dead spirochetes (8, 10). Furthermore, experiments using both inactivated and also noninactivated human serum (data not shown) yielded comparable results in regard to filopodium formation and internalization of borreliae, indicating that complement-dependent killing of spirochetes is probably not a decisive factor for phagocytic uptake of borreliae.

Of note, *B. burgdorferi* spirochetes show remarkable motility *in vivo* (4 μm/s), as determined by intravital imaging of murine tissue (44), and immune cells have to be able to counteract this motility in order to prevent dissemination. *Borrelia*-induced formation of filopodia might thus be a mechanism that allows macrophages to capture highly motile spirochetes within a much larger volume of space than phagocytic events that proceed only at the cell surface (64, 65). Alternatively, both the elongated shape of borreliae as well as their ability to break free from phagocytosing cells by use of their mobility may explain the elaborate capture mechanism used here.

Phagocytosis of a wide variety of bacteria is mediated by TLR, and particularly by TLR2, signaling (66, 67). In particular, (i) phagocytosis of *Listeria* by murine macrophages has been shown to be regulated by a TLR2-MyD88-phosphatidylinositol 3-kinase (PI3K) signaling axis (68), and (ii) MyD88-PI3K signaling, resulting in Arp2/3-dependent actin nucleation, has been demonstrated for phagocytosis of *Borrelia burgdorferi* by murine macrophages (13). Considering that PI3K signaling is central to filopodium formation, including such diverse scenarios as axonal filopodium stimulation by nerve growth factor (69) and herpes simplex virus 1 (HSV-1)-induced filopodium formation during virus uptake (70), it is tempting to speculate that *Borrelia*-stimulated filopodium formation involves a signal cascade involving PI3K-regulated actin nucleation downstream of TLR2-MyD88 signaling. Of note, phagocytic uptake of borreliae is a complex phenomenon that can involve a variety of receptors (10). It is thus to be expected that subsequent signaling events and intracellular processing of borreliae by immune cells may vary accordingly. Still, use of a variety of culture conditions, which may lead to engagement of different receptors, robustly resulted in filopodium/coiling pseudopodium formation in our experiments. However, this phenomenological similarity does not imply that involved receptors or downstream signaling have to be identical in all cases.

Investigating the mechanisms of filopodium extension in live-cell imaging, we detected specific accumulations of GFP-fused forms of the formins FMNL1 and mDia1 at filopodia. Indeed, siRNA-mediated knockdown of FMNL1 and mDia1 demonstrated that both formins are required for efficient formation of filopodia (residual filopodium formation of 50% in cells treated with FMNL1 siRNA and of 25% in cells treated with mDia1 siRNA) and that formin-dependent filopodium formation is closely correlated with the phagocytic index for internalization of borreliae (0.38 for cells treated with FMNL1 siRNA; 0.22 for cells treated with mDia1 siRNA). Both localization of FMNL1 and mDia1 at filopodia and their impact on the formation of these structures are consistent with previous reports, including the recruitment of FMNL1 to filopodial tips of Jurkat T cells or human T cells (39, 46) and the identification of mDia1 as a regulator of filopodium formation in murine neuronal cells (49).

The necessity for both FMNL1 and mDia1 for *Borrelia*-induced filopodia implies respective roles in the generation and/or upkeep of these structures that involve modulation of the actin cytoskeleton. Of note, formins have been described as nucleators of unbranched actin filaments (29, 30, 54, 71, 72). However, biochemical and physiological data imply that the many formins do not (or at least not exclusively) act as actin nucleators but are also involved in the elongation, bundling, or severing of actin filaments (29, 30, 33, 72). Indeed, FMNL1 has been shown to sever actin filaments and to thus generate free barbed ends that are required for Arp2/3 complex-driven actin polymerization during FcγR-mediated phagocytosis of Fc-coated beads by RAW 264.7 cells (73), while mDia1 has been described as an elongation and bundling factor of actin filaments in actin polymerization assays (74, 75). It is thus likely that the requirement of both FMNL1 and mDia1 for coiling phagocytosis of borreliae reflects dual, if not multiple, roles of these formins in the modulation of the macrophage actin cytoskeleton. Moreover, mDia1 has also been shown to interact with microtubules in natural killer cells (76), and both mDia1 and mDia2 act as stabilizers of microtubules in a histone deacetylase 6 (HDAC6)-dependent pathway (77, 78). However, microtubules do not enter into nascent filopodia (79, 80), and a microtubule-associated role of mDia1 in filopodium generation or upkeep is at most expected to be accessory.

Moreover, using fixed specimens, we found that ca. 30% of all uptake events by macrophages proceeded by bona fide coiling phagocytosis. However, based on the high number of ambiguous cases (i.e., without clearly identifiable multiple whorls) we observed, we speculate that the actual proportion of coiling phagocytosis events could actually be twice as high (50% to 60%), which would be consistent with a previous report (8). Combined, these data are consistent with the findings that (i) *Borrelia* uptake by macrophages proceeds to a significant degree by coiling phagocytosis and (ii) FMNL1 and mDia1 are important regulators of this process. Interestingly, F-actin-rich accumulations formed directly at the macrophage surface in response to borreliae were not significantly reduced upon knockdown of either formin (data not shown). These accumulations might indicate con-

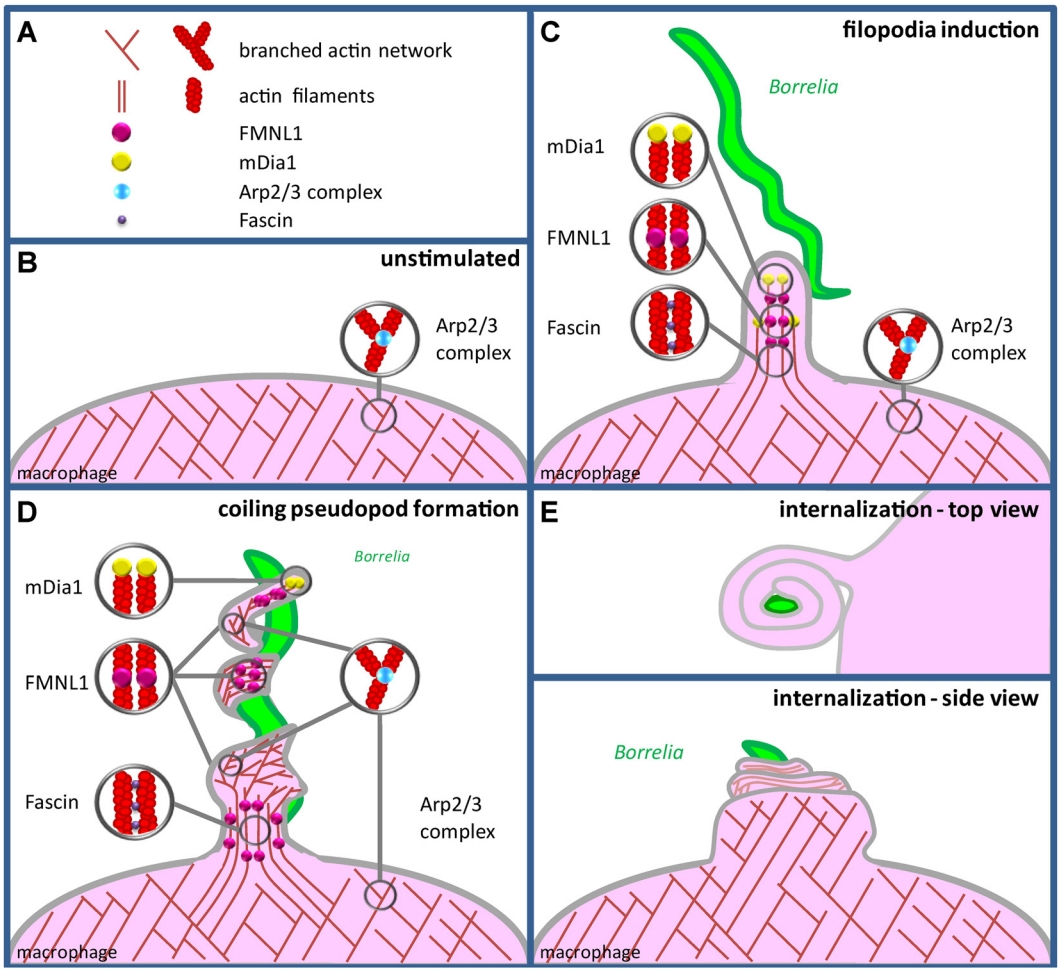

FIG 5 Model of formin- and Arp2/3 complex-dependent actin regulation in coiling phagocytosis of *Borrelia*. (A) The cortical actin network of macrophages contains branched actin networks. (B) Upon stimulation with borreliae, macrophages form filopodial protrusions that arise from the cortical network. Filopodium tips are enriched in the formins FMNL1 and mDia1, which probably contributes to longitudinal growth of filopodia, and contain actin filaments bundled by fascin. (C to E) Upon capturing of a *Borrelia* cell, filopodia enwrap the spirochete. Enwrapping and lateral growth of filopodia into coiling pseudopods are probably enabled by dot-like accumulations of Arp2/3 complex, leading to small, branched actin networks at coiling nodes. Local accumulations of FMNL1 contribute to coiling pseudopod growth by modulating actin filament growth.

ventional phagocytosis events not involving coiling pseudopods that proceed independently of mDia1 or FMNL1. They might also account for the remaining uptake events observed under knockdown of either formin. This form of actin-dependent uptake of borreliae directly at the macrophage surface may involve other formins and/or Arp2/3 complex.

Collectively, our data show that, in addition to Arp2/3 complex, coiling phagocytosis of borreliae by macrophages also requires the formins FMNL1 and mDia1. Interestingly, mDia1 localizes mostly to the tips of *Borrelia*-induced filopodia, while FMNL1 localizes to the tips of filopodia and also along their whole length; Arp2/3 complex is mostly localized in dot-like foci along these protrusions (21). Considering that formins are involved in the generation of unbranched, parallel actin filaments (29, 32, 81) while Arp2/3 complex nucleates branched actin networks (26, 72, 82, 83), we propose the following model for coiling phagocytosis of *Borrelia burgdorferi* by human macrophages (Fig. 5) (i) Upon stimulation with borreliae, macrophages form filopodial protrusions that arise from the cortical actin network. Filopodium tips are enriched in the formins FMNL1 and mDia1, which, by mediating nucleation or remodeling of unbranched actin filaments, contribute to longitudinal growth of filopodia. Moreover, structural stability of filopodia is provided by bundling of actin filaments through fascin. (ii) Upon capturing of a *Borrelia* cell, the filopodium begins to enwrap the spirochete. Enwrapping and concomitant lateral growth of filopodia into coiling pseudopods are probably enabled by dot-like foci of Arp2/3 complex along the entire length of the filopodium, which initiate the formation of branched actin networks at nodes of the developing coiling pseudopod. (iii) Continuous enwrapping and contraction of the coiling pseudopod lead to close contact of the spirochete with the macrophage surface and facilitates subsequent phagocytosis.

This model appears to be in line with earlier observations of (i) the requirement of actin polymerization for the formation of filopodia (62, 81, 84), which is driven at least by mDia1 and mDia2 formins in a variety of cell types (85–88), (ii) the detection of specific accumulations of formins at filopodial tips by fluorescence microscopy (39, 85, 86, 88, 89), (iii) the proposed repetitive

nucleation of actin polymerization at the filopodium tip (60, 62, 80, 84), which is followed by rearrangement/bundling of filaments within the extending filopodial shaft (90), (iv) the localization of Arp2/3 complex-containing dots along filopodia in mouse embryonic fibroblasts (91), and (v) the coexistence of Arp2/3-generated branched networks and longitudinal actin filaments in cell protrusions, as demonstrated by ultrastructural analysis of invadopodia of human metastatic cancer cells (92).

In conclusion, we describe here novel functional and molecular regulatory steps of *Borrelia burgdorferi* coiling phagocytosis that are of key importance for uptake of spirochetes by primary human macrophages. Macrophages respond to contact with borreliae with the formation of fascin-positive filopodia, whose longitudinal growth is driven by the formins FMNL1 and mDia1. *Borrelia*-induced filopodia enable the capturing of spirochetes, which are internalized by lateral growth of filopodia into coiling pseudopods. We conclude that *Borrelia*-induced pseudopod formation during coiling phagocytosis depends not only on the classical actin nucleation machinery involving Arp2/3 complex but also on formin-dependent regulation of actin dynamics. Our data also point to FMNL1 and mDia1 as novel regulators of spirochete uptake by human immune cells.

ACKNOWLEDGMENTS

We thank Arthur Alberts for EGFP-mDia1, Frank Bentzien (UKE Transfusion Medicine) for buffy coats, Daniel Billadeau for YFP-FMNL1 expression constructs, Scott Blystone for EGFP-FMNL1β, George Chaconas for GFP-expressing *B. burgdorferi* strains, Jan Faix for mDia1 antibody, Peter Kraiczy for the *B. burgdorferi* B31 wild-type strain, Bernd Zobiak and Virgilio Failla (UKE Microscopy Facility) and Andrea Mordhorst for expert technical help, and Martin Aepfelbacher for continuous support.

Work in the S.L. lab is funded by the Deutsche Forschungsgemeinschaft (LI925/3-1), Wilhelm Sander-Stiftung (2012.26.1), and the European Union's Seventh Framework Programme (FP7/2007-2013) under grant agreement FP7-237946 (T3Net). M.H. was supported by a junior research grant (NWF-10/05) from the Faculty of Medicine, University of Hamburg.

REFERENCES

1. **Hengge UR, Tannapfel A, Tyring SK, Erbel R, Arendt G, Ruzicka T.** 2003. Lyme borreliosis. Lancet Infect. Dis. **3**:489–500.
2. **Stanek G, Wormser GP, Gray J, Strle F.** 2012. Lyme borreliosis. Lancet **379**:461–473.
3. **Steere AC, Coburn J, Glickstein L.** 2004. The emergence of Lyme disease. J. Clin. Invest. **113**:1093–1101.
4. **Margos G, Vollmer SA, Ogden NH, Fish D.** 2011. Population genetics, taxonomy, phylogeny and evolution of *Borrelia burgdorferi sensu lato*. Infect. Genet. Evol. **11**:1545–1563.
5. **Garcia RC, Murgia R, Cinco M.** 2005. Complement receptor 3 binds the *Borrelia burgdorferi* outer surface proteins OspA and OspB in an iC3b-independent manner. Infect. Immun. **73**:6138–6142.
6. **Hawley KL, Olson CM, Jr, Iglesias-Pedraz JM, Navasa N, Cervantes JL, Caimano MJ, Izadi H, Ingalls RR, Pal U, Salazar JC, Radolf JD, Anguita J.** 2012. CD14 cooperates with complement receptor 3 to mediate MyD88-independent phagocytosis of *Borrelia burgdorferi*. Proc. Natl. Acad. Sci. U. S. A. **109**:1228–1232.
7. **Cinco M, Murgia R, Presani G, Perticarari S.** 1997. Integrin CR3 mediates the binding of nonspecifically opsonized *Borrelia burgdorferi* to human phagocytes and mammalian cells. Infect. Immun. **65**:4784–4789.
8. **Benach JL, Fleit HB, Habicht GS, Coleman JL, Bosler EM, Lane BP.** 1984. Interactions of phagocytes with the Lyme disease spirochete: role of the Fc receptor. J. Infect. Dis. **150**:497–507.
9. **Montgomery RR, Nathanson MH, Malawista SE.** 1994. Fc- and non-Fc-mediated phagocytosis of *Borrelia burgdorferi* by macrophages. J. Infect. Dis. **170**:890–893.
10. **Berende A, Oosting M, Kullberg BJ, Netea MG, Joosten LA.** 2010. Activation of innate host defense mechanisms by *Borrelia*. Eur. Cytokine Netw. **21**:7–18.
11. **Salazar JC, Duhnam-Ems S, La Vake C, Cruz AR, Moore MW, Caimano MJ, Velez-Climent L, Shupe J, Krueger W, Radolf JD.** 2009. Activation of human monocytes by live *Borrelia burgdorferi* generates TLR2-dependent and -independent responses which include induction of IFN-beta. PLoS Pathog. **5**:e1000444. doi:10.1371/journal.ppat.1000444.
12. **Wang G, Ma Y, Buyuk A, McClain S, Weis JJ, Schwartz I.** 2004. Impaired host defense to infection and Toll-like receptor 2-independent killing of *Borrelia burgdorferi* clinical isolates in TLR2-deficient C3H/HeJ mice. FEMS Microbiol. Lett. **231**:219–225.
13. **Shin OS, Miller LS, Modlin RL, Akira S, Uematsu S, Hu LT.** 2009. Downstream signals for MyD88-mediated phagocytosis of *Borrelia burgdorferi* can be initiated by TRIF and are dependent on PI3K. J. Immunol. **183**:491–498.
14. **Hovius JW, Bijlsma MF, van der Windt GJ, Wiersinga WJ, Boukens BJ, Coumou J, Oei A, de Beer R, de Vos AF, van't Veer C, van Dam AP, Wang P, Fikrig E, Levi MM, Roelofs JJ, van der Poll T.** 2009. The urokinase receptor (uPAR) facilitates clearance of *Borrelia burgdorferi*. PLoS Pathog. **5**:e1000447. doi:10.1371/journal.ppat.1000447.
15. **Rittig MG, Krause A, Haupl T, Schaible UE, Modolell M, Kramer MD, Lutjen-Drecoll E, Simon MM, Burmester GR.** 1992. Coiling phagocytosis is the preferential phagocytic mechanism for *Borrelia burgdorferi*. Infect. Immun. **60**:4205–4212.
16. **Horwitz MA.** 1984. Phagocytosis of the Legionnaires' disease bacterium (*Legionella pneumophila*) occurs by a novel mechanism: engulfment within a pseudopod coil. Cell **36**:27–33.
17. **Rittig MG, Jagoda JC, Wilske B, Murgia R, Cinco M, Repp R, Burmester GR, Krause A.** 1998. Coiling phagocytosis discriminates between different spirochetes and is enhanced by phorbol myristate acetate and granulocyte-macrophage colony-stimulating factor. Infect. Immun. **66**:627–635.
18. **Suhonen J, Hartiala K, Viljanen MK.** 1998. Tube phagocytosis, a novel way for neutrophils to phagocytize *Borrelia burgdorferi*. Infect. Immun. **66**:3433–3435.
19. **Cruz AR, Moore MW, La Vake CJ, Eggers CH, Salazar JC, Radolf JD.** 2008. Phagocytosis of *Borrelia burgdorferi*, the Lyme disease spirochete, potentiates innate immune activation and induces apoptosis in human monocytes. Infect. Immun. **76**:56–70.
20. **Wu J, Weening EH, Faske JB, Hook M, Skare JT.** 2011. Invasion of eukaryotic cells by *Borrelia burgdorferi* requires β1 integrins and Src kinase activity. Infect. Immun. **79**:1338–1348.
21. **Linder S, Heimerl C, Fingerle V, Aepfelbacher M, Wilske B.** 2001. Coiling phagocytosis of *Borrelia burgdorferi* by primary human macrophages is controlled by CDC42Hs and Rac1 and involves recruitment of Wiskott-Aldrich syndrome protein and Arp2/3 complex. Infect. Immun. **69**:1739–1746.
22. **Chimini G, Chavrier P.** 2000. Function of Rho family proteins in actin dynamics during phagocytosis and engulfment. Nat. Cell Biol. **2**:E191–E196.
23. **Yi HG, Piao CZ, Kim I, Kim HJ, Oh SY, Kim JW, Kim DY, Lim JH, Seo MD, Park E, Yoon SS, Kim BK, Kim CS, Park S.** 2012. DAAM2 polymorphism is closely related to the clinical outcomes of allogeneic hematopoietic stem cell transplantation. Ann. Hematol. **91**:571–576.
24. **Higgs HN, Pollard TD.** 2001. Regulation of actin filament network formation through ARP2/3 complex: activation by a diverse array of proteins. Annu. Rev. Biochem. **70**:649–676.
25. **Marchand JB, Kaiser DA, Pollard TD, Higgs HN.** 2001. Interaction of WASP/Scar proteins with actin and vertebrate Arp2/3 complex. Nat. Cell Biol. **3**:76–82.
26. **Amann KJ, Pollard TD.** 2001. The Arp2/3 complex nucleates actin filament branches from the sides of pre-existing filaments. Nat. Cell Biol. **3**:306–310.
27. **Park H, Cox D.** 2009. Cdc42 regulates Fc gamma receptor-mediated phagocytosis through the activation and phosphorylation of Wiskott-Aldrich syndrome protein (WASP) and neural-WASP. Mol. Biol. Cell **20**:4500–4508.
28. **May RC, Caron E, Hall A, Machesky LM.** 2000. Involvement of the Arp2/3 complex in phagocytosis mediated by FcγR or CR3. Nat. Cell Biol. **2**:246–248.
29. **Goode BL, Eck MJ.** 2007. Mechanism and function of formins in the control of actin assembly. Annu. Rev. Biochem. **76**:593–627.

30. **Firat-Karalar EN, Welch MD.** 2011. New mechanisms and functions of actin nucleation. Curr. Opin. Cell Biol. **23**:4–13.
31. **Harris ES, Higgs HN.** 2004. Actin cytoskeleton: formins lead the way. Curr. Biol. **14**:R520–R522.
32. **Wallar BJ, Alberts AS.** 2003. The formins: active scaffolds that remodel the cytoskeleton. Trends Cell Biol. **13**:435–446.
33. **Chesarone MA, DuPage AG, Goode BL.** 2010. Unleashing formins to remodel the actin and microtubule cytoskeletons. Nat. Rev. Mol. Cell Biol. **11**:62–74.
34. **Higgs HN.** 2005. Formin proteins: a domain-based approach. Trends Biochem. Sci. **30**:342–353.
35. **Gould CJ, Maiti S, Michelot A, Graziano BR, Blanchoin L, Goode BL.** 2011. The formin DAD domain plays dual roles in autoinhibition and actin nucleation. Curr. Biol. **21**:384–390.
36. **Colucci-Guyon E, Niedergang F, Wallar BJ, Peng J, Alberts AS, Chavrier P.** 2005. A role for mammalian diaphanous-related formins in complement receptor (CR3)-mediated phagocytosis in macrophages. Curr. Biol. **15**:2007–2012.
37. **Seth A, Otomo C, Rosen MK.** 2006. Autoinhibition regulates cellular localization and actin assembly activity of the diaphanous-related formins FRLα and mDia1. J. Cell Biol. **174**:701–713.
38. **Yayoshi-Yamamoto S, Taniuchi I, Watanabe T.** 2000. FRL, a novel formin-related protein, binds to Rac and regulates cell motility and survival of macrophages. Mol. Cell. Biol. **20**:6872–6881.
39. **Gomez TS, Kumar K, Medeiros RB, Shimizu Y, Leibson PJ, Billadeau Daniel D.** 2007. Formins regulate the actin-related protein 2/3 complex-independent polarization of the centrosome to the immunological synapse. Immunity **26**:177–190.
40. **Mersich AT, Miller MR, Chkourko H, Blystone SD.** 2010. The formin FRL1 (FMNL1) is an essential component of macrophage podosomes. Cytoskeleton **67**:573–585.
41. **Han Y, Eppinger E, Schuster IG, Weigand LU, Liang X, Kremmer E, Peschel C, Krackhardt AM.** 2009. Formin-like 1 (FMNL1) is regulated by N-terminal myristoylation and induces polarized membrane blebbing. J. Biol. Chem. **284**:33409–33417.
42. **Shi Y, Zhang J, Mullin M, Dong B, Alberts AS, Siminovitch KA.** 2009. The mDial formin is required for neutrophil polarization, migration, and activation of the LARG/RhoA/ROCK signaling axis during chemotaxis. J. Immunol. **182**:3837–3845.
43. **Goh WI, Ahmed S.** 2012. mDia1-3 in mammalian filopodia. Commun. Integr. Biol. **5**:340–344.
44. **Moriarty TJ, Norman MU, Colarusso P, Bankhead T, Kubes P, Chaconas G.** 2008. Real-time high resolution 3D imaging of the Lyme disease spirochete adhering to and escaping from the vasculature of a living host. PLoS Pathog. **4**:e1000090. doi:10.1371/journal.ppat.1000090.
45. **Barbour AG.** 1984. Isolation and cultivation of Lyme disease spirochetes. Yale J. Biol. Med. **57**:521–525.
46. **Colon-Franco JM, Gomez TS, Billadeau DD.** 2011. Dynamic remodeling of the actin cytoskeleton by FMNL1γ is required for structural maintenance of the Golgi complex. J. Cell Sci. **124**:3118–3126.
47. **Riedl J, Crevenna AH, Kessenbrock K, Yu JH, Neukirchen D, Bista M, Bradke F, Jenne D, Holak TA, Werb Z, Sixt M, Wedlich-Soldner R.** 2008. Lifeact: a versatile marker to visualize F-actin. Nat. Methods **5**:605–607.
48. **Kopp P, Lammers R, Aepfelbacher M, Woehlke G, Rudel T, Machuy N, Steffen W, Linder S.** 2006. The kinesin KIF1C and microtubule plus ends regulate podosome dynamics in macrophages. Mol. Biol. Cell **17**:2811–2823.
49. **Goh WI, Sudhaharan T, Lim KB, Sem KP, Lau CL, Ahmed S.** 2011. Rif-mDia1 interaction is involved in filopodium formation independent of Cdc42 and Rac effectors. J. Biol. Chem. **286**:13681–13694.
50. **Rittig MG, Kuhn KH, Dechant CA, Gauckler A, Modolell M, Ricciardi-Castagnoli P, Krause A, Burmester GR.** 1996. Phagocytes from both vertebrate and invertebrate species use "coiling" phagocytosis. Dev. Comp. Immunol. **20**:393–406.
51. **Rittig MG, Haupl T, Krause A, Kressel M, Groscurth P, Burmester GR.** 1994. *Borrelia burgdorferi*-induced ultrastructural alterations in human phagocytes: a clue to pathogenicity? J. Pathol. **173**:269–282.
52. **Svitkina TM, Borisy GG.** 1999. Arp2/3 complex and actin depolymerizing factor/cofilin in dendritic organization and treadmilling of actin filament array in lamellipodia. J. Cell Biol. **145**:1009–1026.
53. **Welch MD, DePace AH, Verma S, Iwamatsu A, Mitchison TJ.** 1997. The human Arp2/3 complex is composed of evolutionarily conserved subunits and is localized to cellular regions of dynamic actin filament assembly. J. Cell Biol. **138**:375–384.
54. **Chesarone MA, Goode BL.** 2009. Actin nucleation and elongation factors: mechanisms and interplay. Curr. Opin. Cell Biol. **21**:28–37.
55. **Paul AS, Pollard TD.** 2009. Review of the mechanism of processive actin filament elongation by formins. Cell Motil. Cytoskeleton **66**:606–617.
56. **Evangelista M, Zigmond S, Boone C.** 2003. Formins: signaling effectors for assembly and polarization of actin filaments. J. Cell Sci. **116**:2603–2611.
57. **Vignjevic D, Kojima S, Aratyn Y, Danciu O, Svitkina T, Borisy GG.** 2006. Role of fascin in filopodial protrusion. J. Cell Biol. **174**:863–875.
58. **Aratyn YS, Schaus TE, Taylor EW, Borisy GG.** 2007. Intrinsic dynamic behavior of fascin in filopodia. Mol. Biol. Cell **18**:3928–3940.
59. **Mallavarapu A, Mitchison T.** 1999. Regulated actin cytoskeleton assembly at filopodium tips controls their extension and retraction. J. Cell Biol. **146**:1097–1106.
60. **Mattila PK, Lappalainen P.** 2008. Filopodia: molecular architecture and cellular functions. Nat. Rev. Mol. Cell Biol. **9**:446–454.
61. **Gupton SL, Gertler FB.** 2007. Filopodia: the fingers that do the walking. Sci. STKE **2007**:re5. doi:10.1126/stke.4002007re5.
62. **Faix J, Breitsprecher D, Stradal TE, Rottner K.** 2009. Filopodia: Complex models for simple rods. Int. J. Biochem. Cell Biol. **41**:1656–1664.
63. **Rittig MG, Burmester GR, Krause A.** 1998. Coiling phagocytosis: when the zipper jams, the cup is deformed. Trends Microbiol. **6**:384–388.
64. **Aderem A, Underhill DM.** 1999. Mechanisms of phagocytosis in macrophages. Annu. Rev. Immunol. **17**:593–623.
65. **Rittig MG, Wilske B, Krause A.** 1999. Phagocytosis of microorganisms by means of overshooting pseudopods: where do we stand? Microbes Infect. **1**:727–735.
66. **Blander JM, Medzhitov R.** 2004. Regulation of phagosome maturation by signals from Toll-like receptors. Science **304**:1014–1018.
67. **Letiembre M, Echchannaoui H, Bachmann P, Ferracin F, Nieto C, Espinosa M, Landmann R.** 2005. Toll-like receptor 2 deficiency delays pneumococcal phagocytosis and impairs oxidative killing by granulocytes. Infect. Immun. **73**:8397–8401.
68. **Shen Y, Kawamura I, Nomura T, Tsuchiya K, Hara H, Dewamitta SR, Sakai S, Qu H, Daim S, Yamamoto T, Mitsuyama M.** 2010. Toll-like receptor 2- and MyD88-dependent phosphatidylinositol 3-kinase and Rac1 activation facilitates the phagocytosis of *Listeria monocytogenes* by murine macrophages. Infect. Immun. **78**:2857–2867.
69. **Spillane M, Ketschek A, Donnelly CJ, Pacheco A, Twiss JL, Gallo G.** 2012. Nerve growth factor-induced formation of axonal filopodia and collateral branches involves the intra-axonal synthesis of regulators of the actin-nucleating Arp2/3 complex. J. Neurosci. **32**:17671–17689.
70. **Ketschek A, Gallo G.** 2010. Nerve growth factor induces axonal filopodia through localized microdomains of phosphoinositide 3-kinase activity that drive the formation of cytoskeletal precursors to filopodia. J. Neurosci. **30**:12185–12197.
71. **Kovar DR.** 2006. Molecular details of formin-mediated actin assembly. Curr. Opin. Cell Biol. **18**:11–17.
72. **Pollard TD.** 2007. Regulation of actin filament assembly by Arp2/3 complex and formins. Annu. Rev. Biophys. Biomol. Struct. **36**:451–477.
73. **Mason FM, Heimsath EG, Higgs HN, Soderling SH.** 2011. Bi-modal regulation of a formin by srGAP2. J. Biol. Chem. **286**:6577–6586.
74. **Harris ES, Li F, Higgs HN.** 2004. The mouse formin, FRLα, slows actin filament barbed end elongation, competes with capping protein, accelerates polymerization from monomers, and severs filaments. J. Biol. Chem. **279**:20076–20087.
75. **Harris ES, Rouiller I, Hanein D, Higgs HN.** 2006. Mechanistic differences in actin bundling activity of two mammalian formins, FRL1 and mDia2. J. Biol. Chem. **281**:14383–14392.
76. **Butler B, Cooper JA.** 2009. Distinct roles for the actin nucleators Arp2/3 and hDia1 during NK-mediated cytotoxicity. Curr. Biol. **19**:1886–1896.
77. **Bershadsky AD, Ballestrem C, Carramusa L, Zilberman Y, Gilquin B, Khochbin S, Alexandrova AY, Verkhovsky AB, Shemesh T, Kozlov MM.** 2006. Assembly and mechanosensory function of focal adhesions: experiments and models. Eur. J. Cell Biol. **85**:165–173.
78. **Destaing O, Saltel F, Gilquin B, Chabadel A, Khochbin S, Ory S, Jurdic P.** 2005. A novel Rho-mDia2-HDAC6 pathway controls podosome patterning through microtubule acetylation in osteoclasts. J. Cell Sci. **118**:2901–2911.
79. **Schober JM, Komarova YA, Chaga OY, Akhmanova A, Borisy GG.**

2007. Microtubule-targeting-dependent reorganization of filopodia. J. Cell Sci. **120**:1235–1244.
80. **Svitkina TM, Bulanova EA, Chaga OY, Vignjevic DM, Kojima S, Vasiliev JM, Borisy GG.** 2003. Mechanism of filopodia initiation by reorganization of a dendritic network. J. Cell Biol. **160**:409–421.
81. **Mellor H.** 2010. The role of formins in filopodia formation. Biochim. Biophys. Acta **1803**:191–200.
82. **Goley ED, Welch MD.** 2006. The ARP2/3 complex: an actin nucleator comes of age. Nat. Rev. Mol. Cell Biol. **7**:713–726.
83. **Welch MD, Mullins RD.** 2002. Cellular control of actin nucleation. Annu. Rev. Cell Dev. Biol. **18**:247–288.
84. **Faix J, Rottner K.** 2006. The making of filopodia. Curr. Opin. Cell Biol. **18**:18–25.
85. **Peng J, Wallar BJ, Flanders A, Swiatek PJ, Alberts AS.** 2003. Disruption of the Diaphanous-related formin Drf1 gene encoding mDia1 reveals a role for Drf3 as an effector for Cdc42. Curr. Biol. **13**:534–545.
86. **Pellegrin S, Mellor H.** 2005. The Rho family GTPase Rif induces filopodia through mDia2. Curr. Biol. **15**:129–133.
87. **Peng GE, Wilson SR, Weiner OD.** 2011. A pharmacological cocktail for arresting actin dynamics in living cells. Mol. Biol. Cell **22**:3986–3994.
88. **Schirenbeck A, Bretschneider T, Arasada R, Schleicher M, Faix J.** 2005. The diaphanous-related formin dDia2 is required for the formation and maintenance of filopodia. Nat. Cell Biol. **7**:619–625.
89. **Block J, Breitsprecher D, Kuhn S, Winterhoff M, Kage F, Geffers R, Duwe P, Rohn JL, Baum B, Brakebusch C, Geyer M, Stradal TE, Faix J, Rottner K.** 2012. FMNL2 drives actin-based protrusion and migration downstream of Cdc42. Curr. Biol. **22**:1005–1012.
90. **Medalia O, Beck M, Ecke M, Weber I, Neujahr R, Baumeister W, Gerisch G.** 2007. Organization of actin networks in intact filopodia. Curr. Biol. **17**:79–84.
91. **Johnston SA, Bramble JP, Yeung CL, Mendes PM, Machesky LM.** 2008. Arp2/3 complex activity in filopodia of spreading cells. BMC Cell Biol. **9**:65. doi:10.1186/1471-2121-9-65.
92. **Schoumacher M, Goldman RD, Louvard D, Vignjevic DM.** 2010. Actin, microtubules, and vimentin intermediate filaments cooperate for elongation of invadopodia. J. Cell Biol. **189**:541–556.